

Ruth G. Hidalgo-Hernandez*, Nayomi Plaza and Oscar Marcelo Suárez

A study on tribological characterization of Al-Cu-Mg-B composites subjected to mechanical wear

Abstract: Tribological properties of a series of aluminum matrix composites reinforced with AlB_2 particles developed for lightweight machinery parts intended for aerospace and automotive applications were evaluated. In this study, the worn surfaces of aluminum matrix composites containing copper and magnesium with different amounts of reinforcing AlB_2 dispersoids were examined by scanning electron microscopy to determine the effects of a pin-on-disk wear test. These observations also allowed identification of the probable wear mechanisms involved upon wearing against a martensitic stainless steel ball. The effect of chemical composition on the wear volume and wear coefficient was measured to establish the relationship between the reinforcing diboride content and matrix conditions and the corresponding wear response.

Keywords: AlB_2 ; aluminum matrix composites; tribology; wear characterization; wear testing.

*Corresponding author: Ruth G. Hidalgo-Hernandez, US Patent and Trademark Office, 401 Dulany Street, Alexandria, VA 22314, USA, Phone: +1-787-342-1500, e-mail: hidalgo.ruth@gmail.com

Nayomi Plaza: Materials Science Program, University of Wisconsin-Madison, 1509 University Avenue, Madison, WI 53706, USA

Oscar Marcelo Suárez: Department of General Engineering, University of Puerto Rico-Mayagüez, PO Box 9000, Mayagüez, PR 00681-9000, Puerto Rico

1 Introduction

In mechanical design, it is important to take into account wear produced in any system, especially for certain aerospace and automotive applications, wear being defined as the progressive loss of material due to the relative motion between a solid surface and a contacting substance or surface. Wear can be affected by sliding loads, impact loads, speed, and temperature, among other parameters. The variation of these parameters as well as the material nature greatly affect the wear mechanisms experienced by the surface. Normally the mechanisms are classified as abrasive, adhesive, oxidative, tribofilm, and delamination deformations associated with single or repeated contacts. Combination of adhesive wear and abrasive wear followed

by oxidative and tribofilm mechanisms is the most dominant in engineering situations [1].

In recent years, metal matrix composites became widely used because of their excellent mechanical and wear resistance properties. In this category, a series of high-strength, lightweight aluminum matrix composites (AMCs), particularly those reinforced with AlB_2 particles, have been developed for aerospace applications [2]. Those composites containing Cu can be further strengthened by convenient precipitation hardening treatments, similar to unreinforced Al-Cu alloys. The high hardness attained in these Al/ AlB_2 composites made them attractive particularly for high-wear parts where low density is also a requirement [3]. AMCs subject to dry wear conditions usually experience severe adhesive wear as well as abrasion along with deformations associated with contact followed by chemical mechanisms such as oxidative wear. Adhesive wear takes place when actual contacts between sliding surfaces occur at discrete points, forming bonds that are broken and created at new locations until fracture occurs within a weaker asperity. Abrasive wear, also known as single-cycle deformation mechanism associated with sliding motion, occurs when a harder body deforms a softer one, causing displacement, loss of material, or both during a single engagement. Wear mechanisms are likely to coexist, although usually one of them dominates the wear situation. For instance, abrasive wear often concurs with oxidative wear and delamination wear, which is observed as displacement of material along the sliding direction. In order to reduce the wear rate to a satisfactory level, lubricants are widely used [1]. Pin-on-disk wear testing represents a simple simulation of the wear response of an AMC under normal operating conditions, as the environmental conditions can be easily controlled [4].

2 Experimental procedure

2.1 Materials selection and processing

The composite fabricated consisted of a matrix made of a ternary Al-Cu-Mg alloy reinforced with hard aluminum diboride particles. In the production of the composites

through gravity casting, three commercial master alloys were used: Al-5 wt% B, Al-10 wt% Mg, and Al-33 wt% Cu. Magnesium and copper were used as alloying elements because of their high solubility in the Al solid solution [5], which contributes greatly to the overall wear resistance of the Al-B-Cu-Mg composites. In each composite the aluminum matrix was composed of Al-2.5 wt% Cu-1 wt% Mg. The AlB_2 particles (contained in the Al-B master alloy) were used as reinforcement for the composite matrix, with the amount of boron ranging from 0 to 4 wt%. The size of the AlB_2 particles, the volume percent of particles, and volume percent of pores were studied in a prior research on AMCs with the same composite compositions [6]. These AlB_2 particles ranged in size from 1 to 20 μm . The volume percent of particles increases with the weight percent of boron, varying from 1.4% to 16%. The same tendency is shown in the volume percent of pores that varies from 0.37% to 2.30% with the increase in the amount of boron [6].

The charge material was mixed and melted in an electrical furnace at 750°C to avoid the transformation from AlB_2 to AlB_{12} [2, 7, 8]. In the process, AlB_2 particles tend to be at the bottom of the graphite crucible because of higher density (3.2 g/cm³) than liquid aluminum (~2.4 g/cm³) at the furnace operating temperature. Therefore, to attain more homogeneity of the samples, mechanical agitation was applied with a stirring rod, while the molten composite, containing solid boride particles, was poured into a cylindrical preheated graphite mold. Graphite was used because of its high thermal conductivity to favor high solidification rates and smaller grains.

After solidification, the 2-inch-diameter ingots were annealed at 350°C for 4 h in an electrical furnace. The power of the furnace was turned off to allow the ingots to cool to room temperature. The purpose of the annealing treatment was to homogenize the chemical composition of the matrix and to stabilize the microstructure of the fabricated composites, avoiding the influence of the stress concentrations due to uneven cooling rates in the castings [6]. Al-Cu-Mg matrix composites could have been strengthened by means of an aging treatment. However, samples were annealed only because we wanted to study the wear rate solely as a function of their chemical composition and not their heat treatability.

The ingots were sectioned with a low-speed saw and disk specimens were obtained. The specimens were mounted, ground, and polished to produce a flat, scratch-free surface for metallographic analysis. The grinding steps included 320, 400, 600, 800 grit SiC papers. The samples were polished using 3- μm diamond suspension followed by a 0.05- μm SiO_2 emulsion. Finally, the samples were cleaned with distilled water and alcohol and dried to be characterized.

2.2 Materials characterization

The composite microstructure was investigated using optical microscopy (OM), scanning electron microscopy (SEM), and energy-dispersive spectroscopy (EDS). For OM, the samples were observed using a Nikon (Melville, NY, USA) Epiphot 200 inverted optical microscope, and the SEM analysis was performed with a JEOL (Peabody, MA, USA) 6390 scanning electron microscope.

Dry sliding wear test was conducted using a pin-on-disk tester where the composite samples were the disks and a 440 martensitic stainless steel ball with a diameter of 3 mm was the indenting pin. The setup consisted of the indenting pin resting on the composite sample disk, rotating under the influence of a load. The apparatus was constructed in our research laboratory on the basis of specifications of the ASTM G99 standard. Low contact loads and small sliding velocity were selected to offset excessive heating in the samples. The test was conducted twice at each condition with a 1 N constant load at a 0.004-m/s sliding speed and a total sliding distance of 2.5 m, using a new pin for each test. The worn surfaces and wear debris were analyzed using SEM (equipped with an EDS system) and OM. Optical profilometry using a Zygo (Middlefield, CT, USA) New View 6300 profilometer system allowed determination of the geometry (depth and width) of the pin-on-disk tracks, which permitted us to determine the material volume removed due to wear.

3 Results

3.1 Microstructure analysis

Microstructure analysis of the composites without etching allowed the identification of the phases, using the microstructure analyses of previous research with similar compositions as a reference. A homogeneous distribution of particles was obtained and the thermodynamically stable θ phase was identified [6]. The five optical micrographs in Figure 1 evince the distribution of reinforcement particles in the matrix as boron level increases in the composite from 0 to 4 wt%. These micrographs show diborides embedded in the aluminum matrix that appear as darker particles and distributed in clusters throughout the entire matrix [9]. In Figure 1A, the intermetallic phase, Al_2Cu (θ), homogenized through annealing, is evident throughout the matrix but mainly in the matrix grain boundaries. The metastable θ' is not present because aging was not performed in these specimens [10].

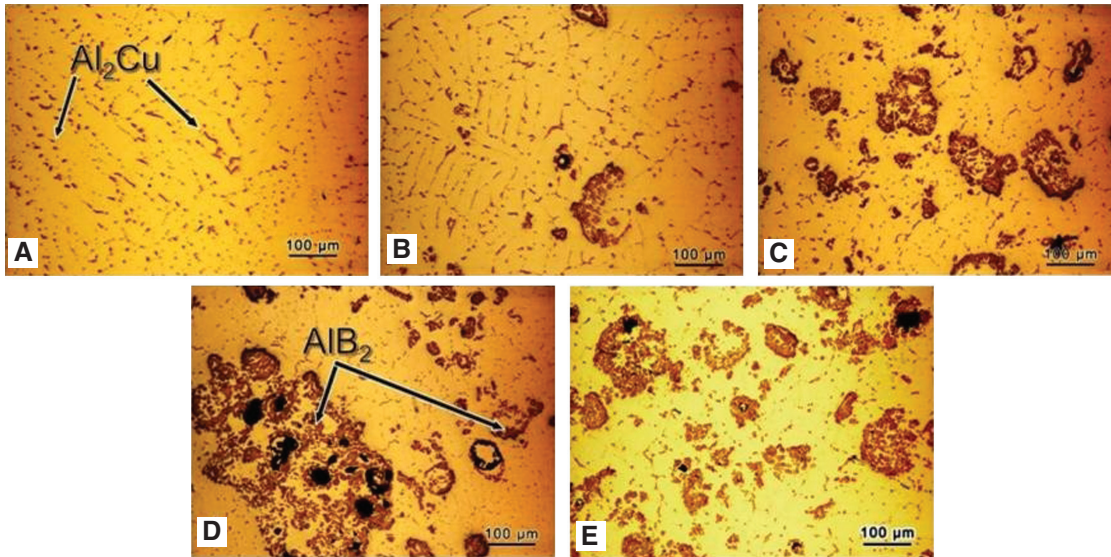


Figure 1 Optical micrographs showing the AlB_2 distribution as boron levels increase from 0 to 4 wt%: (A) Al-2.5 wt% Cu-1 wt% Mg-0 wt% B, (B) Al-2.5 wt% Cu-1 wt% Mg-1 wt% B, (C) Al-2.5 wt% Cu-1 wt% Mg-2 wt% B, (D) Al-2.5 wt% Cu-1 wt% Mg-3 wt% B, (E) Al-2.5 wt% Cu-1 wt% Mg-4 wt% B.

Then, the samples were observed with a SEM equipped with an EDS system (Figure 2). It should be noted that the boron $K\alpha$ peak was at the fringe of the EDS detection limit (low-energy side of the EDS spectrum). However, the microstructure analysis revealed the presence of boron in the composites. Figure 2A shows a secondary electron image of the microstructure of Al-2.5 wt% Cu-1 wt% Mg-2 wt% B composite, where an elliptical cluster of AlB_2 is apparent. Figure 2B shows a global EDS spectrum revealing the presence of copper, magnesium, and aluminum in the Al-2.5 wt% Cu-1 wt% Mg-2 wt% B composite.

3.2 Wear characteristics

Tribological experiments were focused on the determination of wear measured by the material volume removed, the wear coefficient value, and the material removal rates. The calculation of wear volume on each sample was based on topographical analysis via optical profilometry techniques, taking into consideration the track width, depth, and perimeter. Figure 3 evinces the differences in wear volume among samples. Noticeably, for higher boron concentrations (i.e., more AlB_2 particles), the wear volume decreases. Moreover, the wear volume of the unreinforced alloy is greater than that of the composites containing diboride particles.

For all of the composites under the same testing conditions, we calculated the values of the wear coefficient based on the worn volume obtained with the track geometry (maximum depths and widths), as measured by

optical profilometry. The wear coefficient was evaluated using Eq. (1) proposed by Archard [11], where the wear volume (V) is directly proportional to the sliding distance (d) and the applied normal force (F), by the dimensional wear coefficient (k), conventionally in units of $\text{mm}^3/\text{N}\cdot\text{m}$. The resulting experimental wear coefficients are presented in Figure 4 as a function of boron percent. All the composites exhibited similar behavior with increasing content of AlB_2 , where the wear coefficient decreases in the composites, obtaining higher wear resistance. This behavior is visibly related to the wear volume measured.

$$V = kFd \quad (1)$$

Archard's wear equation can be modified to Preston's equation [12–15] to calculate the material removal rate (RR) or dV/dt . According to Preston's equation [Eq. (2)], the relative velocity (v_r) between the spherical pin and the specimen surface, the applied normal load (F), and the time (t) are the main parameters determining the amount of material removal (dV). Table 1 shows the variation of RR as a function of boron levels, showing the same tendencies as in wear volume.

$$\text{RR} = dV/dt = kFv_r \quad (2)$$

3.3 Microscopy analysis of worn surfaces

SEM examination revealed detailed information on the wear tracks and debris, pointing to the formation of parallel scratches with plastic deformation edges. For instance,

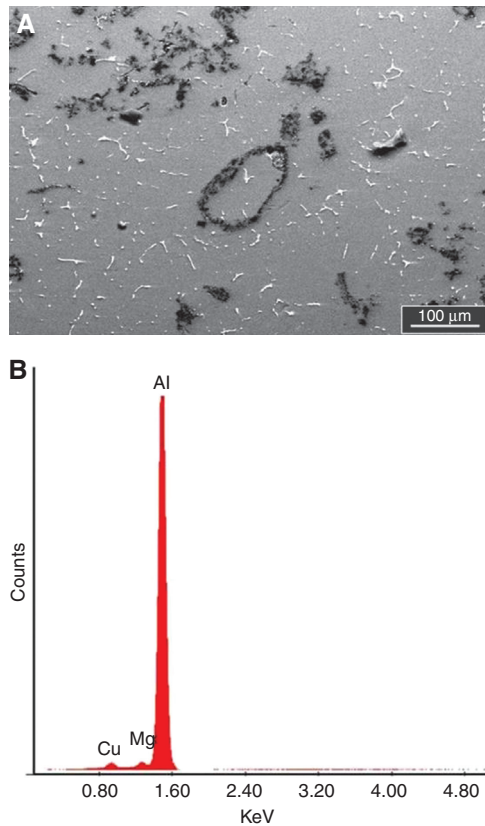


Figure 2 (A) SEM image of Al-2.5 wt% Cu-1 wt% Mg-2 wt% B, (B) Global EDS spectrum of the worn surface detected in Al-2.5 wt% Cu-1 wt% Mg-2 wt% B composite.

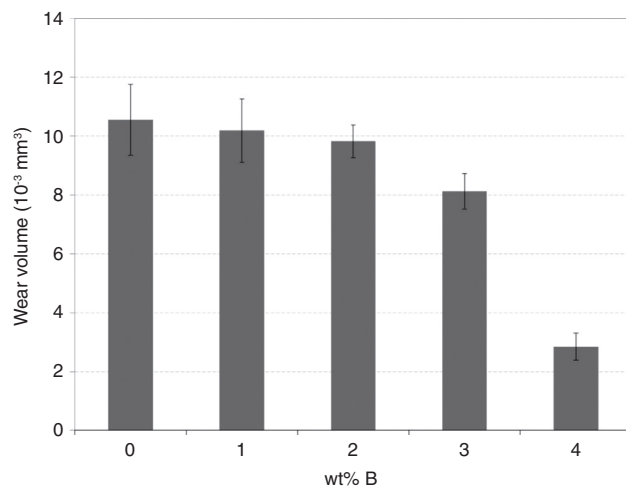


Figure 3 Wear volume measured using optical profilometry as a function of boron percent.

Figure 5 showed that the pin-on-disk wear test carried out on the Al-Cu-Mg-B composites induced plastic deformation, ploughing, and deposition of debris onto the surface. These features were accompanied by many grooves along

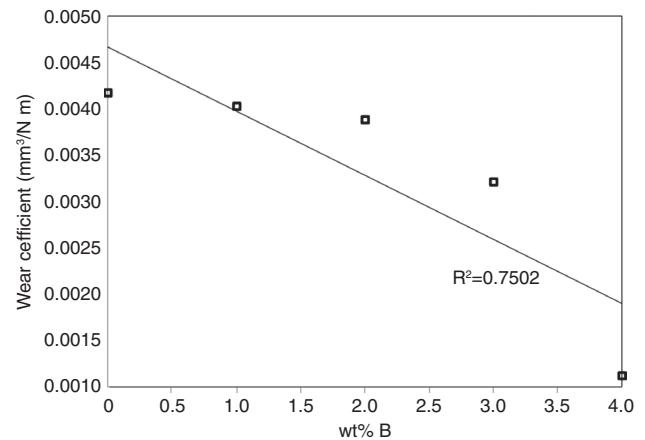


Figure 4 Wear coefficient measured on the tested samples as a function of boron content in the composites.

Table 1 Removal rate as function of boron percentage in the samples.

B, wt%	Material removal rate, mm ³ /s
0	1.75871×10^{-5}
1	1.73157×10^{-5}
2	1.73181×10^{-5}
3	1.39348×10^{-5}
4	4.67133×10^{-6}

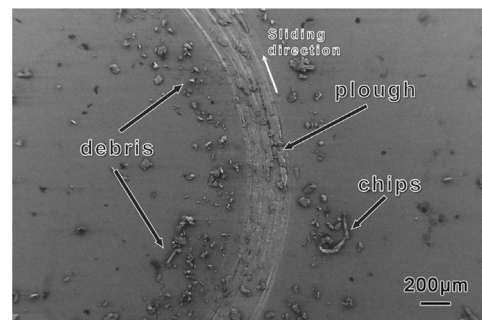


Figure 5 SEM micrographs of pin-on-disk worn surface on Al-2.5 wt% Cu-1 wt% Mg-0 wt% B composite.

the sliding direction, while the peeling of the matrix formed worn chips that adhered to the composite surface.

SEM images reveal that AlB_2 particles are uniformly distributed throughout the matrix alloy. In our SEM observations coupled with EDS analysis, we discovered that the diboride particles hide themselves under the worn surface [16]. Other investigators have proposed that particle reinforcements are the most effective in improving the wear resistance of AMCs [17] by providing good interfacial bonding between the reinforcement and the matrix. The resistance to plastic flow becomes visible at places where

clusters of AlB_2 are located, as seen in Figure 6. Figure 7 shows EDS spectrum analysis of the wear track where the presence of Fe was absent, resulting in no evidence of adhesive wear. The EDS analysis proved the nonappearance of debris coming from the pin, i.e., stainless steel, as no adhered pin material was found on the wear track, confirming the discovery in a previous research [18].

Through further inspection of the SEM images, diverse wear mechanisms were identified: oxidative

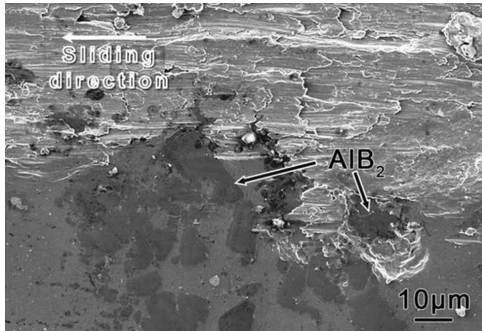


Figure 6 SEM images showing evidence of resistance to plastic flow of Al-2.5 wt% Cu-1 wt% Mg-1 wt% B composite.

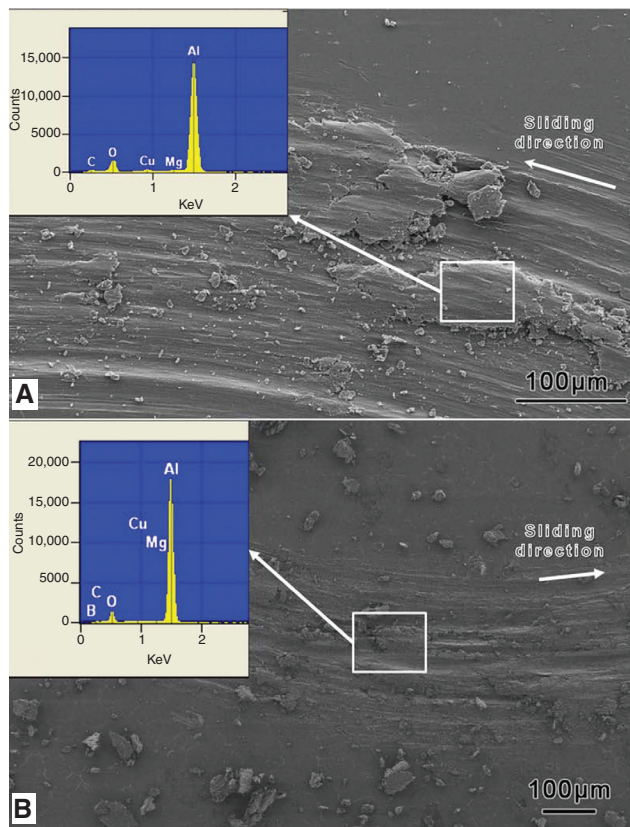


Figure 7 EDS spectrum analysis of wear track: (A) Al-2.5% Cu-1% Mg-0% B composites, (B) Al-2.5% Cu-1% Mg-3% B composite.

wear, abrasion wear, and delamination wear. Figure 8, A and B, show oxygen concentration of an X-ray mapping analysis on Al-2.5% Cu-1% Mg-0% B and Al-2.5% Cu-1% Mg-3% B wear tracks, respectively. These characteristics, along with the oxygen peaks present in the EDS spectrum shown in Figure 7, indicate an oxidative wear mechanism, in which unlubricated conditions of sliding cause relatively high “hot-spot” temperatures at the surface, producing oxidation [19]. Figure 9 corroborates the abrasive wear mechanism by illustrating the appearance of grooves and damage spots forming ploughs on the worn surface. Evidence of delamination wear on the composite surface can be seen in Figure 10, showing the presence of induced cracks when repeated and constant sliding introduces dislocations in the subsurface by plastic deformation that eventually shears the surface and forms long thin flake debris [20]. Furthermore, the wear tracks showed a change in the dominant wear mechanism present in the composite from abrasive wear to delamination wear when the level of boron rises from 3 to 4 wt%, as evidenced by the flake debris shown with arrows in Figure 11.

4 Discussion

The results exposed a clear dependence of the wear resistance of the composites on the amount of reinforcement particles present in the samples. The literature corroborated that ceramic-reinforced AMCs have better wear resistance than the unreinforced alloys [21]. The composites with 0 wt% (unreinforced alloy) to 2 wt% B are characterized by higher wear rates, which translates into lower wear resistance with respect to the composites with higher levels of boron. As aforementioned, it is evident that the presence of AlB_2 particles reduces the wear volume and wear coefficient of the composites. Based on the literature, the addition of hard ceramic particles improves the wear resistance of the composites by preventing direct metallic contacts that induce subsurface deformation [22]. As the content of AlB_2 increases in the composites, decreasing wear is observed as a result of the strong bonding (attachment) of the particles with the matrix during sliding wear conditions. The aluminum matrix surrounding the particles is worn away first, and essentially all contact remains between the reinforcing particles and the steel counterface (indenting pin). We can then attribute the enhanced wear strength to a combination of the supporting effect of the matrix to the diboride particles in addition to the strong Al/ AlB_2 interface bond [23]. This strong attachment of the particles to the aluminum was observed in prior research where similar composites were subjected to impact loads [2].

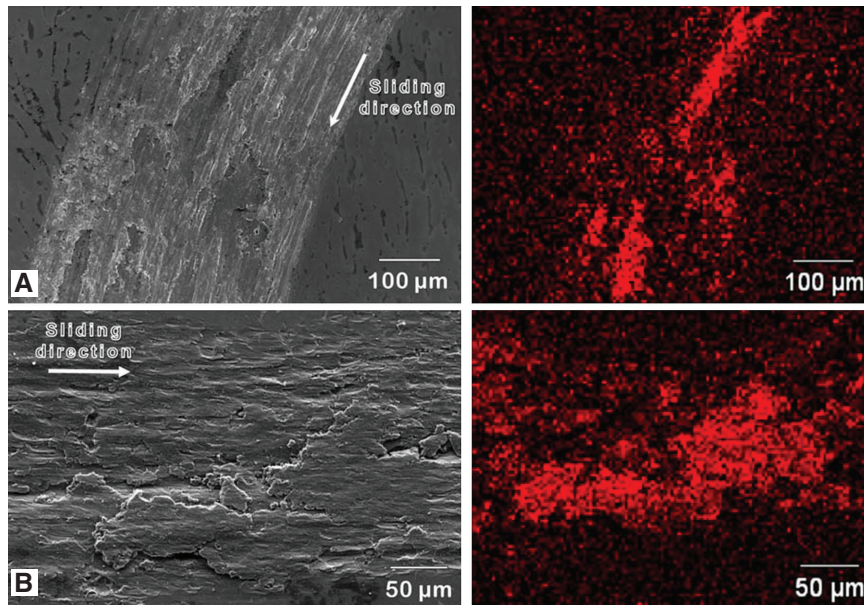


Figure 8 SEM micrographs and oxygen elemental map of: (A) Al-2.5% Cu-1% Mg-0% B, (B) Al-2.5% Cu-1% Mg-3% B.

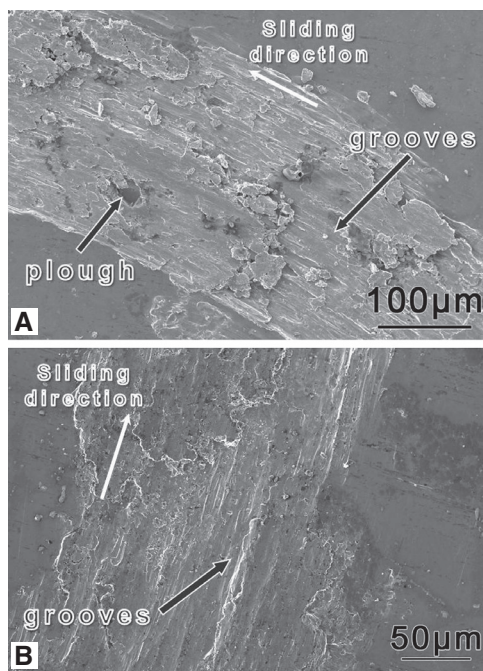


Figure 9 SEM micrograph evidence of grooves and ploughs due to abrasive wear: (A) Al-2.5% Cu-1% Mg-1% B composite and (B) Al-2.5% Cu-1% Mg-3% B composite.

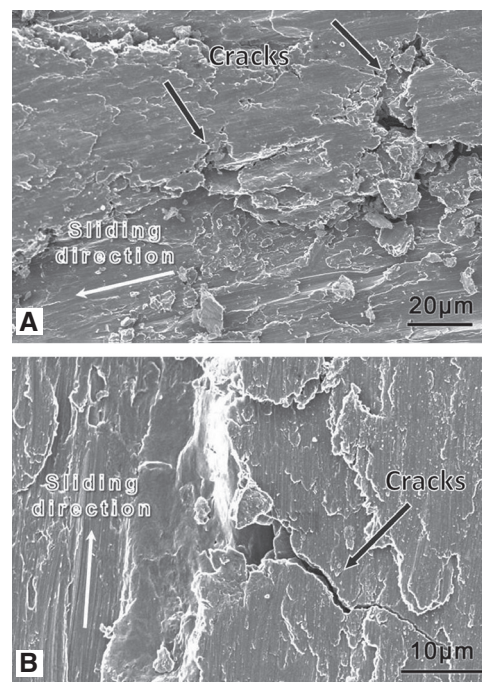


Figure 10 SEM micrographs showing induced cracks (arrows): (A) Al-2.5% Cu-1% Mg-1% B composite, (B) Al-2.5% Cu-1% Mg-3% B composites.

The reduction of wear coefficient in the Al-Cu-Mg-B composites with increased content of AlB_2 particles can be attributed to the improvement in antifrictional behavior of reinforced particles that act as the load-bearing elements [24]. As a consequence, our results demonstrate that the reinforcement particles play a more direct role in the

wear behavior of the composites. The SEM observations and EDS analysis revealed that the diboride particles hide themselves under the worn surface [16], showing a resistance to plastic flow concentrated near clusters of AlB_2 (Figure 6). Nonetheless, we deem essential to produce additional observations to fully characterize the wear

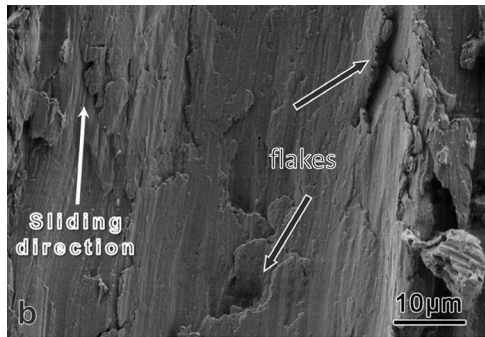


Figure 11 SEM showing evidence of delamination wear damage (arrows) in Al-2.5 wt% Cu-1 wt% Mg-3 wt% B composite.

mechanisms involved under more demanding wear conditions, i.e., higher loads and longer sliding distances.

5 Conclusions

On the basis of the results obtained, we can conclude that the wear volume and wear coefficient of the Al-Cu-Mg composites tend to decrease for higher concentrations of AlB_2 particles in the composites. The lowest wear volume and wear coefficient were reached in Al-B-Cu-Mg composites containing 4 wt% boron. Observations of the pin-on-disk tracks revealed that three wear mechanisms

exist: oxidative wear, abrasive wear, and delamination wear. Consequently, AlB_2 particles play a direct role in the wear behavior of the composite: As the increment of boron levels in the composites affects the wear behavior of the composites, a resulting enhancement of wear resistance in the composites is obtained.

Acknowledgments: This research was based upon work supported by the NSF under Grant No. 0351449 (PREM Program) and HRD 0833112 (CREST Program). The authors would like to acknowledge the support provided by the Puerto Rico Louis Stokes Alliance for Minority Participation Bridge to the Doctorate Program under NSF grant HRD 0601843. AMG Aluminum (Wayne, PA, USA) facilitated the Al-B master alloys, whereas AMBIOS Tech provided some wear track analysis. Gratitude is given to professors Jayanta Banerjee and Paul Sundaram from the Department of Mechanical Engineering, University of Puerto Rico-Mayaguez (UPRM) for their essential feedback. This research would not have been successful without the assistance and collaboration of UPRM mechanical engineering undergraduate students Carlos Osorio and Alexis Torres, and Dr. Hermes Calderón as well as Humberto Melgarejo and Dr. Kumar Sridharan from the University of Wisconsin-Madison.

Received December 26, 2012; accepted July 23, 2013; previously published online August 21, 2013

References

- [1] Bayer RG. In *Wear Analysis for Engineers*, HNB Publishing: New York, 2002, pp. 29–41.
- [2] Suárez OM. *J. Mech. Behav. Mater.* 2001, 12, 225–237.
- [3] Korkut MH. *Mater. Sci. Technol.* 2004, 20, 73–81.
- [4] Zhang J, Alpas AT. *Scr. Metall. Mater.* 1992, 26, 505–509.
- [5] Rohatgi P. *Metal Matrix Composite and Method of Producing*, EP805726, 1997.
- [6] Calderon H. *Effect of Cyclic High Loading Rates on the Fatigue Strength of Aluminum-Based Composites*, PhD thesis, University of Puerto Rico-Mayaguez, Puerto Rico, 2009.
- [7] Suárez OM, Yupa-Luna J, Calderón HE. *Trans. Am. Foundry Soc.* 2003, 111, 159–166.
- [8] Calderón H. *Effects of Mechanical Deformation on Aluminum Matrix Composite Heat-Treated*, MS thesis, University of Puerto Rico-Mayaguez, Puerto Rico, 2004 (in Spanish).
- [9] Wang X. *J. Alloys Compd.* 2005, 403, 283–287.
- [10] Fujima T, Tanaka A, Yoshimura S, Takagi K. *J. Phys.: Conf. Ser.* 2009, 176, 012045.
- [11] Archard JF. *J. Appl. Phys.* 1953, 24, 981–988.
- [12] Maney RT, Brown NJ, Baker PC. *Proc. SPIE* 1981, 306, 41–57.
- [13] Gessenharter A, Brinksmeier E, Riemer O. *J. Precis. Eng.* 2006, 30, 325–336.
- [14] Kasai T. *Tribol. Int.* 2008, 41, 111–118.
- [15] Neuroth N, Bach H. *The Properties of Optical Glass*, Springer Verlag: New York, NY, USA, 1998.
- [16] Iwai Y, Miyajima T. *Wear* 2003, 255, 606–616.
- [17] Modi OP, Prasad BK, Yegneswaran AH, Vaidya ML. *Mater. Sci. Eng. A* 1992, 151, 235–245.
- [18] Sridharan K, Melgarejo ZH, Suarez OM. *Composites, Part A* 2008, 39, 1150–1158.
- [19] Ludema KC. In *ASM Handbook: Friction, Lubrication and Wear Technology*, ASM International: Novelt, OH, 2004, Vol. 18, pp. 175–329.
- [20] Abrahamson EP, Suh NP, Jahanuir S. *The Delamination Theory of Wear*. National Technical Information Service, US Department of Commerce: Washington, DC, USA, 1974.
- [21] Veeresh Kumar GB, Rao CSP, Selvaraj N. *J. Miner Mater. Charact. Eng.* 2011, 10, 59–91.
- [22] Zhang J, Alpas AT. *Mater. Sci. Eng. A* 1993, 161, 273–284.
- [23] Lu D, Zhou R, Jiang Y. *Wear* 2003, 255, 134–138.
- [24] Ramesh CS, Keshavamurthy R, Channabasappa BH, Pramod S. *Tribol. Int.* 2010, 43, 623–634.